SPACE WEATHER, VOL. 11, 1–13, doi:10.1002/swe.20065, 2013

Prediction of extreme geomagnetically induced currents in the UK high-voltage network

Ciarán D. Beggan,[1] David Beamish,[1] Andrew Richards,[2] Gemma S. Kelly,[1] and Alan W. P. Thomson[1]

Received 15 March 2013; revised 11 June 2013; accepted 13 June 2013.

[1] Geomagnetically Induced Currents (GIC) can be damaging to high-voltage power transmission systems. GIC are driven by rapid changes in the strength of the magnetic field external to the Earth's surface. Electric fields are produced in the ground by the interaction between this changing magnetic field, the sea and the conductivity structure of the Earth. Using a technique known as the "thin-sheet approximation," we can determine the electric field at the Earth's surface, which in turn allows the calculation of GIC in the earthing connections of high-voltage transformers within a power grid. We describe two new developments in the modeling of GIC in the UK, though the results are applicable to GIC-related research in other regions. Firstly, we have created an updated model of the UK surface conductivity by combining a spatial database of the UK geological properties (i.e., rock type) with an estimate of the conductivity for specific formations. Secondly, we have developed and implemented a sophisticated and up-to-date model for the 400 kV and 275 kV electrical networks across the whole of Great Britain and, in addition, the 132 kV network in Scotland. We can thus deduce the expected GIC at each transformer node in the system based on the network topology from an input surface electric field. We apply these developments to study the theoretical response of the UK high-voltage power grid to modeled extreme 100 year and 200 year space weather scenarios and to a scaled version of the October 2003 geomagnetic storm, approximating a 1 in 200 year event.

Citation: Beggan, C. D., D. Beamish, A. Richards, G. S. Kelly, and A. W. P. Thomson (2013), Prediction of extreme geomagnetically induced currents in the UK high-voltage network, *Space Weather*, *11*, doi:10.1002/swe.20065.

1. Introduction

[2] Large excess electric fields are generated in the ground during severe space weather events due to the (secondary) induction effects of a changing magnetic field within a conductive medium. During large geomagnetic storms, electric currents—termed Geomagnetically Induced Currents (GIC)—can flow through the ground, usually harmlessly. However, high-voltage power systems can be vulnerable to GIC flow, particularly where they offer a low-resistance path for the current compared to the ground (for a recent overview, see *Radasky* [2011]). In this paper, we seek to simulate the flow of GIC in the UK high-voltage network using a state-of-the-art ground conductivity model and the most accurate and up-to-date representation of the grid characteristics and topology available.

[3] The key magnetic parameter in the "GIC problem" is the time rate of change of the magnetic field, denoted $d\mathbf{B}/dt$, and in particular its component in the horizontal plane, $d\mathbf{B}_H/dt$ [e.g., *Viljanen et al.*, 2001]. Determining the expected peak rate of change of $d\mathbf{B}_H/dt$ for a region is important for GIC studies. Values of $d\mathbf{B}_H/dt$ can be readily extracted from digital archives, typically recorded at a cadence of 1 min. *Thomson et al.* [2011] estimated likely 100 year and 200 year maxima in $d\mathbf{B}_H/dt$ using up to 30 years of minute-mean digital data from 28 European observatories. They showed that peak $d\mathbf{B}_H/dt$ increases with magnetic latitude, with a distinct "bump" in the magnitude of $d\mathbf{B}_H/dt$ around 55°N–60°N (geomagnetic latitude), associated with an enhanced ionospheric current system known as the auroral electrojet. The UK is within this region of enhanced magnetic field activity and so experiences such enhancements during major geomagnetic storms.

[4] Prior to 1983 in the UK, only analogue measurements recorded on paper exist, though these do extend back to the 1840s and contain major magnetic storms such

[1]British Geological Survey, Edinburgh UK.
[2]Market Operation, National Grid Ltd, Wokingham, Berkshire, UK.

Corresponding author: C. D. Beggan, British Geological Survey, Murchison House, West Mains Road, Edinburgh EH9 3LA, UK. (ciar@bgs.ac.uk)

1542-7390/13/10.1002/swe.20065

as the "Carrington Event" of September 1859 and the May 1921 storm (e.g., as discussed in *Kappenman* [2006]). In the digital era, severe magnetic storms occurred in March 1989, November 1991, and October 2003. In the UK, the 1989 storm caused damage to two transformers [*Smith*, 1990; *Erinmez et al.*, 2002a, 2002b].

[5] Detailed geophysical studies of these storms, such as *McKay* [2003] and *Turnbull* [2010, 2011], have modeled the impact on simplified versions of the high-voltage transmission system of the UK. *Thomson et al.* [2005] showed that the measured GIC for the 2003 event was reasonably reproduced by the geophysical models of *Beamish et al.* [2002] and *McKay* [2003], which were constructed for the UK mainland (also known as Great Britain (GB)) but were most detailed in Scotland. Measured GIC (three phases summed) in the UK during the October 2003 event reached 40 A [*Thomson et al.*, 2005]. Note, all GIC values quoted are in Amps for a three phase neutral. More recently, *Pulkkinen et al.* [2012] have developed scenarios of realistic electric field change for a 100 year extreme event, specifically to aid engineering and network planning. These were applied to the high-voltage network of Virginia in the USA and also to a relatively simple model of the GB high-voltage network to compute the expected GIC in the network. However, these were relatively uniform electric field models and lacked the expected spatial variation of the magnetic and induced electric field. In this paper, we attempt to produce a more realistic representation of the induced electric field in the UK during a severe space weather event and use an improved network model to compute the expected GIC for the GB power grid.

[6] In section 2, we describe our new conductivity model which is based on the geophysical properties of the geological structure of the UK. We then describe the methodology for creating the extreme variations of the magnetic field during 100 year and 200 year extreme geomagnetic events using synthetic models of the auroral electrojet and a scaled version of the October 2003 storm. In section 3, we show the resulting GIC amplitudes and spatial patterns generated when applied with our new model of the high-voltage transmission network. Finally, we discuss the limitations and caveats with regard to modeling accuracy and validation.

2. GIC Modeling

[7] There are four main requirements for computing GIC within an electrical network: (a) a model of the conductivity structure of the region, (b) a detailed set of spatial and temporal measurements and/or models of the magnetic field, (c) the computation of the electric field from the interaction of (a) and (b), and (d) a network model of the high-voltage power grid and transformers.

[8] Once the surface electric field has been computed, the voltages along electrical lines in a connected power grid are integrated and inverted using the network topology and characteristics to calculate GIC at each transformer. These four steps are described in more detail in the following subsections.

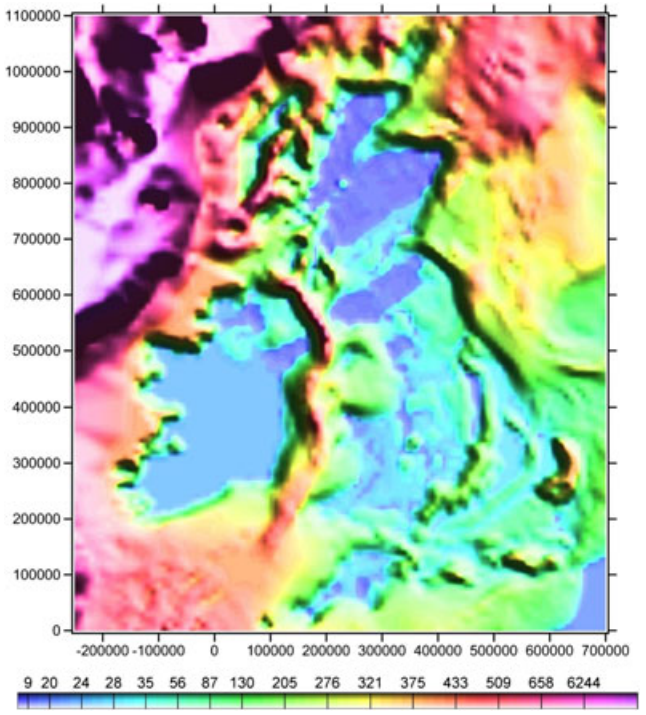

Figure 1. Conductance model (in S, 10 km resolution) of the UK based on the inferred conductivity of rock units in the British Geological Survey 1:625,000 geological database. Axis coordinates are in British National Grid (Units: m). Image uses shaded-relief (from NE) to emphasize gradients.

2.1. UK Ground Conductivity Model

[9] The penetration of the magnetic field into the ground (i.e., skin depth) is highly dependent on the conductivity of the local region and the time period (frequency) over which the change of the magnetic field occurs. The vertical distribution of the resistivity within the Earth's crust, and the period considered, determine the rate of attenuation of the induced electric field. Deeper layers are more significant at long periods, and the shallow layers produce stronger influences at short periods.

[10] The interaction of the external magnetic field with the conductive Earth is approximated in our code by "thin-sheet" modeling; this determines the surface electric field arising at a particular frequency from layers of conductive material in the subsurface. The chosen frequency (or period) of the rate of change of the magnetic field is related to its penetration depth.

[11] The thin-sheet modeling code used in this study is based upon the work of *Vasseur and Weidelt* [1977]. Using a series of appropriate Green's functions and integrals, the thin-sheet approximation can be used to model the influence of near surface conductivity contrasts in the

Table 1. Estimated 100 and 200 Year Maxima in $d\mathbf{B}_H/dt$ and $\mathbf{B}_H$ Between 55° and 60° Geomagnetic North Summarized From *Thomson et al.* [2011], Figures 5 and 6

	$d\mathbf{B}_H/dt$ (nT/min)	$\mathbf{B}_H$ (nT)
100 year return	1000–4000	2000–5000
200 year return	1000–6000	3000–6500

context of regional induction. Hence, a thin-sheet model includes the effect that lateral conductivity variations have on redistributing regional or "normal" currents induced elsewhere (e.g., oceans or shelf seas). The surface layer can be regarded as a sheet of finite laterally variable conductance, across which certain boundary conditions apply. A horizontal magnetic field will induce an electric field in the subsurface which creates a discontinuity current sheet at the surface. Hence, the thin-sheet model includes the effect that lateral conductivity variations will have on redistributing regional currents induced elsewhere. In addition to the surface layer, the model also includes a lower half-space with a resistivity of 900 Ω m to model the upper and lower crust and mantle.

[12] The new UK thin-sheet conductivity model is derived from the analysis of the conductivity properties of the bedrock materials, based on the British Geological Survey (BGS) 1:625,000 geological map of the UK and Northern Ireland. The model, described by *Beamish* [2012], uses the information obtained from recent airborne geophysical surveys across the UK to compute the conductance to a depth of 3 km. The results show that the effective resistivity mapped from remote sensing surveys can be used to estimate conductivity across most of the UK. The methodology (see also *Beamish and White* [2012]) provides a lithological and geostatistical assessment of the conductivities of all the UK bedrock formations. The central moments of the distributions were found to range from 8 to 3125 Ω m.

[13] There are a number of assumptions in this method, not all of which are strictly true. For example, the assumption that surface bedrock extends to depth or that rock units (sandstone, limestone, basalt, etc) have uniform and constant conductivities to a depth of 3 km are clearly incorrect in many locations. However, the approximations are useful in constructing a reasonably representative regional conductivity model.

[14] Onshore, the 1:625,000 "near-surface" bedrock conductivities were used including Northern Ireland but excluding the Republic of Ireland. For the offshore regions, the bathymetry and a uniform value of sea water conductivity (4 S/m) are used. This is, on average, a very thin layer (typically < 200 m) providing a conductance which matches the conditions of a previous existing thin-sheet model from March 2002. Figure 1 shows the model, termed the BGS2012 Conductivity Model. At the 10 km cell size used, the model comprises 4211 values of conductance, ranging from 2 to 11598 S.

2.2. Regional Estimation of the Magnetic and Electric Fields

[15] The temporal variation of the external magnetic field during a severe geomagnetic storm can be extremely rapid with a complex regional spatial variation. In the auroral regions, results from networks of magnetometers such as International Monitor for Auroral Geomagnetic Effects (IMAGE) [*Viljanen and Häkkinen*, 1997] or Canadian Array for Realtime Investigations of Magnetic Activity (CARISMA) [*Mann et al.*, 2008] show rapid temporal fluctuations and spatial rearrangement of the magnetic field associated with auroral electrojets and field-aligned currents.

[16] In order to estimate the surface electric field, we must make assumptions about the configuration of the magnetic field during a large storm at the geomagnetic latitudes of the UK. We therefore assume that strong magnetic fields arise primarily from the presence of a very strong auroral electrojet expanding southward over the UK, driven by a major geomagnetic storm. We assume the auroral electrojet generates a rapidly changing external magnetic field observed on the ground. The core and crustal magnetic fields are essentially static on short time scales of seconds to days, and we ignore the effect of the ring current as the electrojet is the largest signal at these latitudes during such events. The rapidly changing external part of the magnetic field induces an electric field in the Earth, and we use the horizontal, North (X) and East (Y), components to compute a regional surface electric field model.

[17] Two different scenarios for the spatial and temporal configuration of the magnetic field were synthesized: (a) a set of idealized models of a large-scale auroral electrojet and (b) a scaled version of the 2003 Halloween storm based

Table 2. Static Input Fields to the Conductivity Model[a]

Return Period (Years)	$d\mathbf{B}_H/dt$ (nT/min)	1/Frequency (min)	Electrojet Field Strength H_0 (nT)
30	1000	2	450
30	1000	10	2275
30	1000	30	3820
100	3000	2	1350
100	3000	10	(6825)
200	5000	2	2250
200	5000	10	(11,375)

[a] H_0 of 6825 nT and 11,375 nT are regarded as relatively unlikely physical scenarios but are included for completeness.

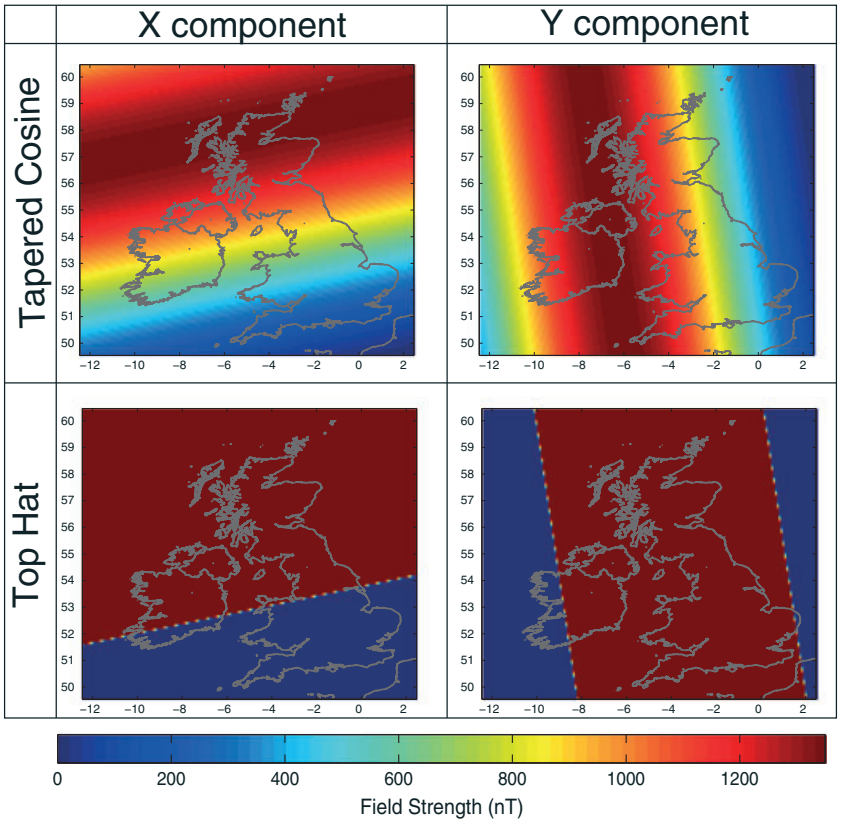

Figure 2. The horizontal components of the magnetic field from an extreme electrojet configuration.

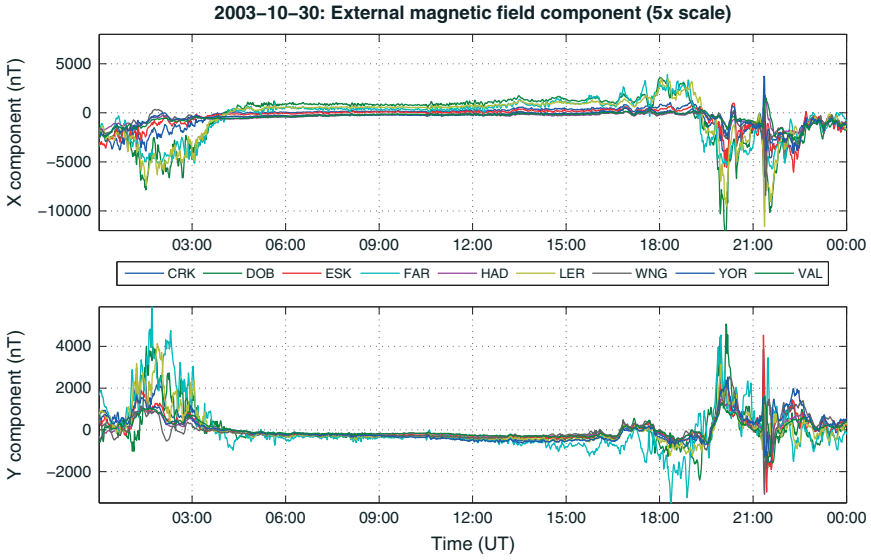

Figure 3. Time series of the 5×-scaled horizontal components of the external magnetic field from the Halloween storm of 30 October 2003 geomagnetic storm. The data come from the following observatories and variometers in the region. CRK: Crooktree, DOB: Dombres, ESK: Eskdalemuir, FAR: Faroes, HAD: Hartland, LER: Lerwick, WNG: Wingst, YOR: York, VAL: Valentia.

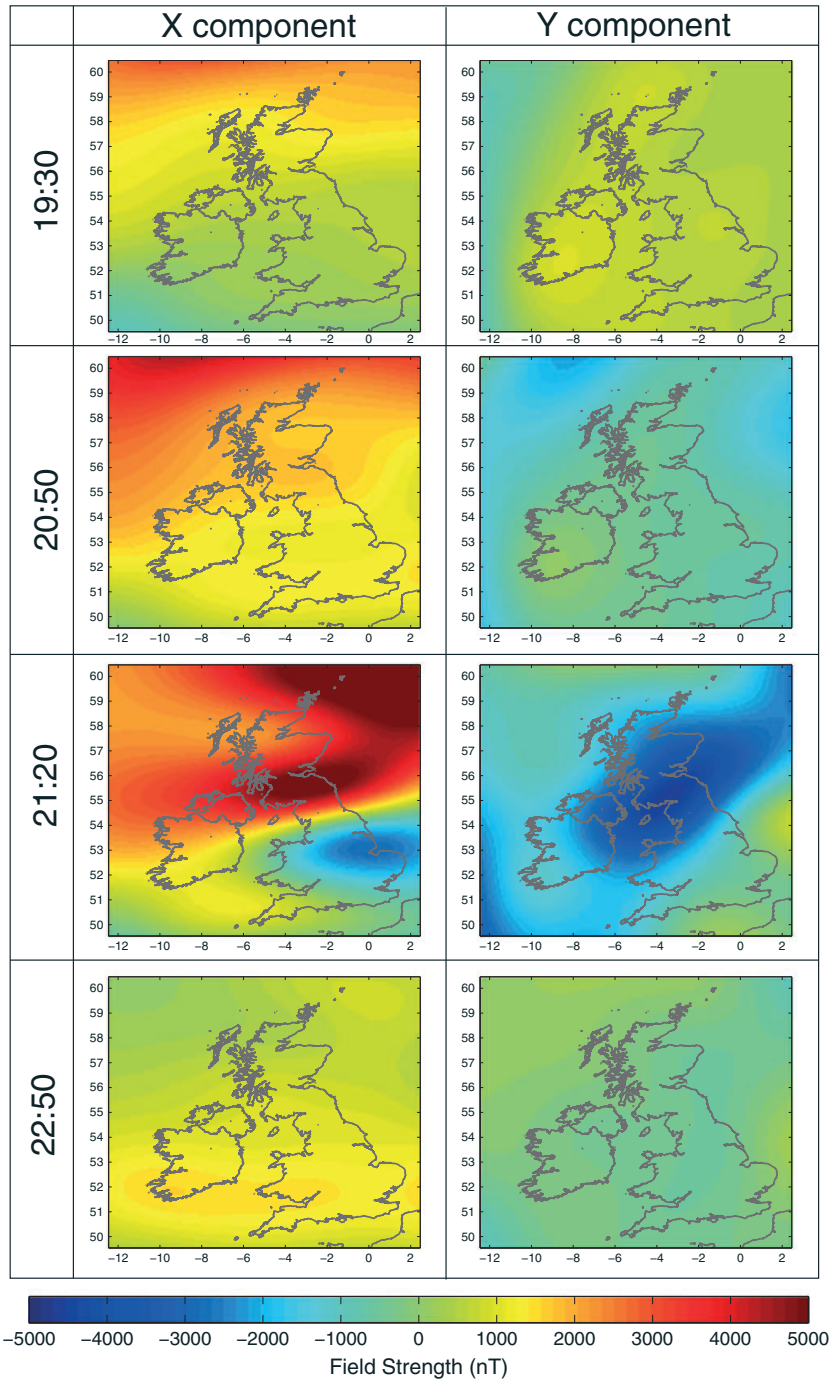

Figure 4. Snapshot of the horizontal components of the magnetic field from an extreme (approximately ×5) version of the Halloween storm of 30 October 2003 geomagnetic storm. The columns show the (left) X component and the (right) Y component. Nominal times in UT.

on the interpolation of the magnetic field from observatory and variometer measurements around the UK.

2.2.1. Electrojet Models

[18] We developed two electrojet model profiles: the first electrojet model has an amplitude profile akin to a "top-hat" function, extending from 53°N to 63°N in geomagnetic latitude, while the second has a "tapered-cosine" profile extending between 48°N and 68°N in geomagnetic latitude. We use the two different models to examine if the amplitude gradient (slope) of the magnetic field strongly affects the GIC. The Top-Hat model gives a very strong gradient across its edges while the

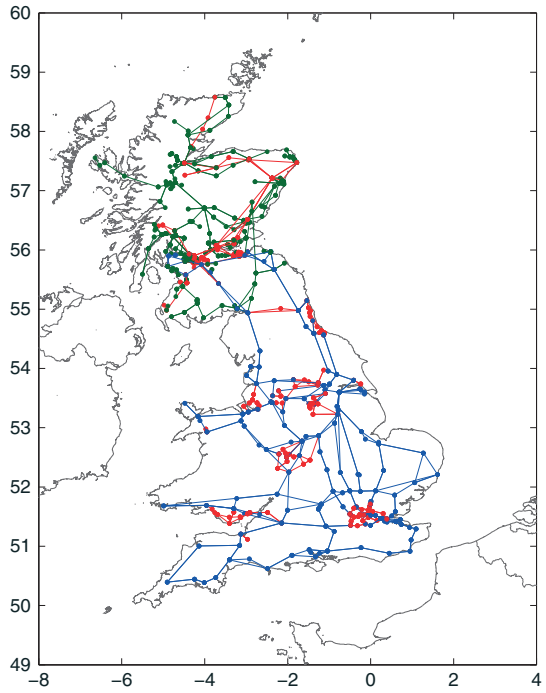

Figure 5. Network map of the National Grid GB high-voltage power grid containing 1317 transformers (dots) and 1178 connections (lines). Blue: 400 kV; red: 275 kV; green: 132 kV (Scotland only). Note, many sites host multiple transformers and connecting power lines run in parallel.

Tapered-Cosine model has a gentler gradient. Two orientations of the auroral electrojet were then computed: (a) geomagnetically east-west aligned across the UK and in order to produce an orthogonal magnetic field direction, (b) a second set of profiles in a geomagnetic north-south alignment (which approximately follow the central axis of the UK). Note that a north-south configuration is not realistic due to the configuration of the main magnetic field.

[19] The electrojet models were created as normalized values on a square grid in geomagnetic coordinates and then rotated 10° counter-clockwise to match the appropriate position over the UK in geographic coordinates. The electrojet grids were cropped and sub-sampled to 1/12th of a degree to match the grid-spacing of the ground conductivity model.

[20] To scale the electrojet model, magnetic fields to the correct amplitude for an extreme event, the results from the *Thomson et al.* [2011] study on the statistical predictions of extreme values in European magnetic observatory data were applied. Table 1 gives the predicted range in activity between 55°N and 60°N at 100 year and 200 year return periods. The largest measured digital (i.e., modern) $d\mathbf{B}_H/dt$ for the UK is around 1100 nT/min (in 1991). Therefore, we chose to use 1000 nT/min, 3000 nT/min, and 5000 nT/min in this analysis to approximate the expected maximum in $d\mathbf{B}_H/dt$ for 30, 100, and 200 years.

[21] To convert the horizontal rate of change to equivalent root-mean-square (RMS) input horizontal field for use in the thin-sheet approximation code, we assumed the field amplitude was changing sinusoidally over a period of length t. Hence the RMS input field strength, H_0, can be computed using the approximation:

$$d\mathbf{B}_H/dt = \sqrt{2}\pi H_0/T \quad (1)$$

where $\mathbf{B}_H = H_0 \sin(2\pi t/T)$. H_0 is the strength of the field from the electrojet and T is the period of electrojet variation (in minutes). If we assign T = 2 min, this leads to magnetic field input strengths H_0 of approximately 450 nT, 1350 nT, and 2250 nT for $d\mathbf{B}_H/dt$ = 1000 nT/min, 3000 nT/min, and 5000 nT/min. The conductivity model responds differently at different periods (or frequencies) to these magnetic field changes. For this study, the response of the electric field at periods of 2 min (120 s), 10 min (600 s), and 30 min (1800 s) are chosen, though the spectral characteristics of the external magnetic field during storms are typically broadband in nature. Longer periods are regarded as insignificant for GIC hazard assessment.

[22] *Thomson et al.* [2011] suggest that in Europe the extremes in $\mathbf{B}_H$ are relatively unlikely to exceed 10,000 nT once every 200 years. We therefore use this as a maximum cut-off for the value of H_0. For this reason, 3000 nT/min and 5000 nT/min changes are not considered to be physically reasonable as "worst cases" for electrojets varying with periods longer than about 10 min. However, we do retain them for comparison purposes.

[23] We assume that the change in $\mathbf{B}_H$ is due either to the X or the Y component of the external magnetic field. Table 2 shows the computed values for the horizontal component of the main field corresponding to these time periods for the electrojet models.

[24] There are now up to 12 different magnetic field source scenarios for electric field computation per time period: (a) two electrojet profiles (Top Hat and Tapered Cosine), (b) two orientations (as geomagnetically E-W and N-S aligned electrojets), and (c) two or three $d\mathbf{B}_H/dt$ scaling values (as per Table 2). The grid models were multiplied by the selected H_0 values to scale them to the magnetic field strength before combining them with the conductivity model to calculate the electric field strength at each point across the UK mainland. Figure 2 shows an example of the magnetic field strength for the auroral electrojets models scaled to 1350 nT (a 1-in-100 year scenario). For convenience, we concentrate on the 120 s period for the remainder of the paper, though the models for all scenarios were computed.

2.2.2. Scaled October 2003 Storm

[25] To generate a more "realistic" representation of the spatial variation of the geomagnetic field during a large storm, a model of the magnetic field during the October 2003 event was constructed based upon the measurements from nine observatories and variometers around the United Kingdom and North Sea region. The observatory

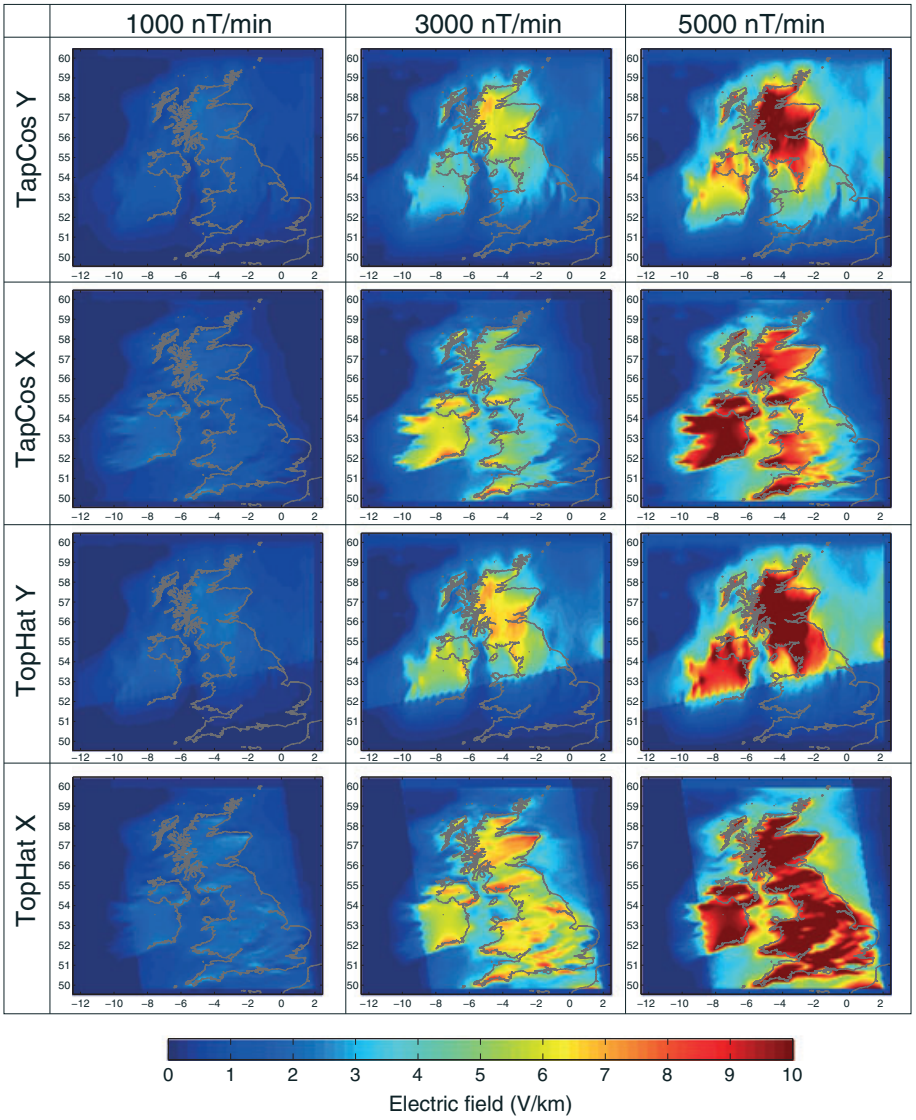

Figure 6. Electric field induced in the surface for a period of 120 s due to an H_0 field of (left) 450, (middle) 1350, and (right) 2250 nT from an auroral electrojet model with a Tapered-Cosine or Top-Hat function in an East-West (X) or North-South (Y) aligned configuration.

data were downloaded from the World Data Centre for Geomagnetism (Edinburgh), while the Faroes, York, and Crooktree variometer data were provided by the Sub-Auroral Magnetometer Network (SAMNET) operated by Lancaster University.

[26] The spatial variation of the magnetic field was estimated using minute-mean data interpolated over a large region using the Spherical Elementary Current Systems method [*Amm and Viljanen*, 1999], as described in detail in *McLay and Beggan* [2010]. For each minute of the day, the magnetic field values were multiplied by five to achieve a 200 year extreme event with a peak maximum rate of change of approximately 5000 nT/min. Figure 3 illustrates the variation at each observatory/variometer of the (scaled) horizontal components of the external magnetic field for the 30 October 2003. The magnetic field was most active during the period 19.00–22.00 UT. Figure 4 shows the spatial change of the strength of the horizontal field components for four snapshots, including 21.20 UT, the peak of the 2003 Halloween storm, as recorded in the UK. The magnetic field then was assumed to have a particular dominant frequency (e.g., 120 s), from which a set of electric field models were computed. The electric field models were used to derive GIC across the electrical network at each minute of the day.

2.3. UK High-Voltage Network Model

[27] National Grid UK is responsible for the operation of the high-voltage 400 kV, 275 kV, and 132 kV transmission network across Great Britain (i.e., the mainland

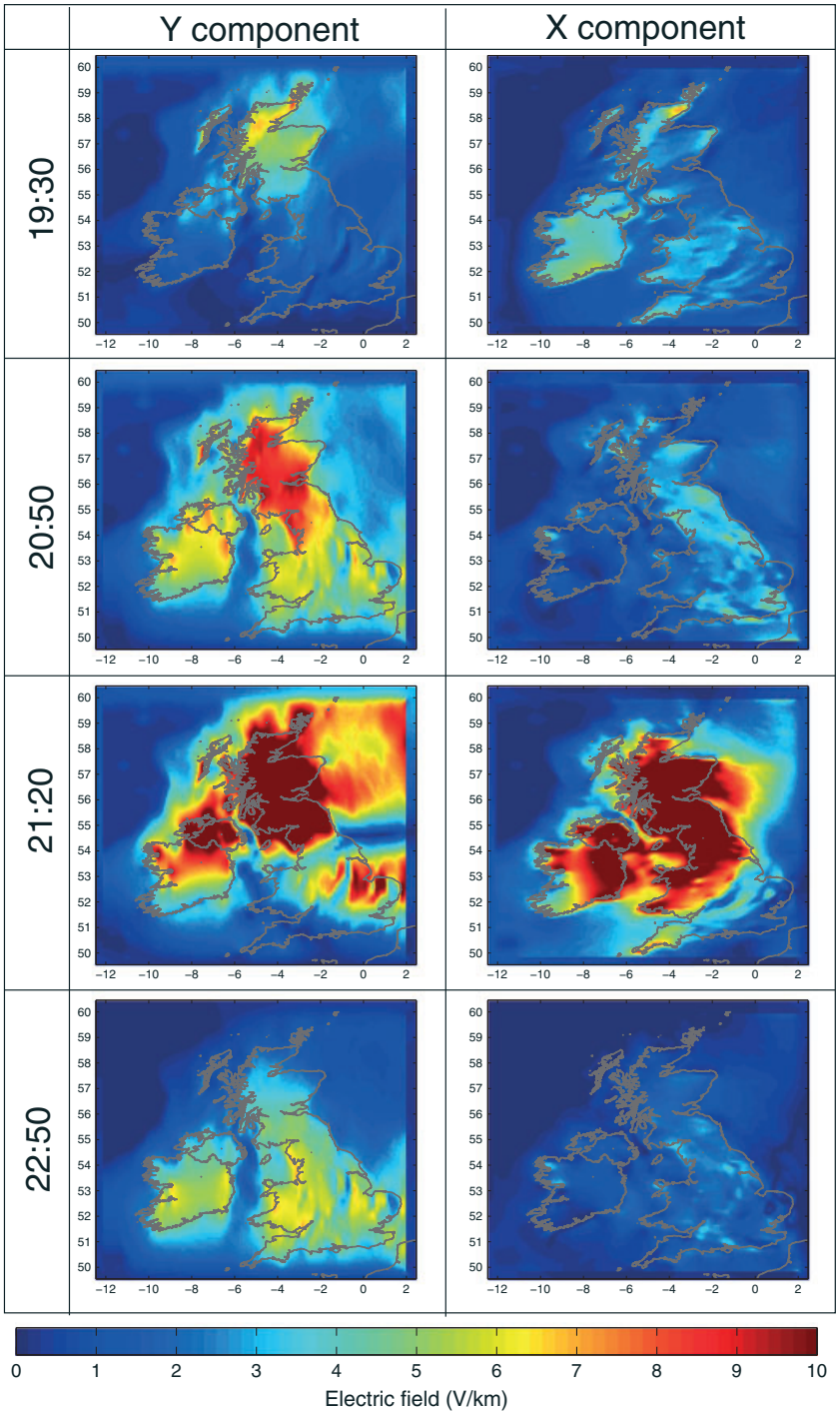

Figure 7. Electric field induced in the surface for period of 120 s due to magnetic fields from an extreme version of the 30 October 2003 geomagnetic storm. The columns show the (left) *Y* component and the (right) *X* component. Nominal times (in UT) are illustrative, taken from the time profile of the October 2003 storm.

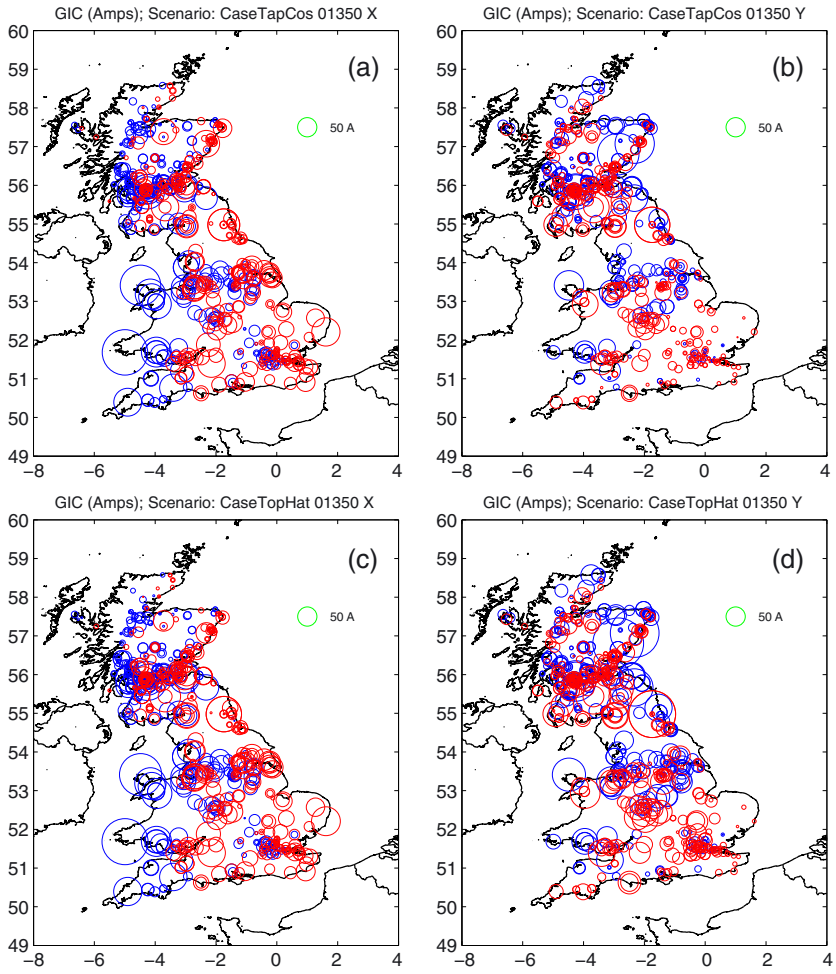

Figure 8. GIC in the National Grid GB high-voltage network due to a 100 year extreme scenario (120 s period) from an auroral electrojet with the following configurations: (a) Tapered Cosine East-West aligned, (b) Tapered Cosine North-South aligned, (c) Top Hat East-West aligned, and (d) Top Hat North-South aligned. Blue indicates GIC directed into the grid, red indicates GIC into the ground. Circle size represents size (relative to scale). Note that many sites have multiple transformers present.

of the UK). The transmission network consists of hundreds of step-up and step-down transformers that transfer power generated typically at 22.5 kV from the source to the local distribution networks for industrial, business, and household consumers. The most efficient method for transferring power over long distances is to step the voltage up to reduce the resistance (and hence the Ohmic heating) in the connecting transmission lines. However, if the ground resistance is sufficiently high, the low-resistance wires of the network provide an easier route for GIC to pass through the earth neutral of the connecting transformers.

[28] In conjunction with National Grid UK, a full description of the UK high-voltage power network was developed. The data consists of latitude, longitude, and electrical characteristics (earthing, transformer and line resistance) of each transformer node in the high-voltage network. These parameters are used to calculate GIC (in Amperes) along power transmission lines from the matrix equation in *Lehtinen and Pirjola* [1985]:

$$\mathbf{I} = (\mathbf{Y} + \mathbf{Z})^{-1}\,\mathbf{J} \tag{2}$$

where $\mathbf{J}$ is the geo-voltage computed between nodes, $\mathbf{Z}$ is the impedance matrix, $\mathbf{Y}$ is the network admittance matrix and $\mathbf{I}$ is the vector containing the estimated GIC at each node. The input data from the network parameters are used to calculate $\mathbf{Y}$ and $\mathbf{Z}$. The geo-voltage $\mathbf{J}$ is calculated by interpolating the electric field grid value onto the power transmission lines and integrating along the line. The GIC at each node on the grid is then computed. The GIC are calculated from both the North and East components of the surface electric field. Note that when modeling real-world data, to compute the total GIC at each node, all periods should be integrated. In this study, however, we

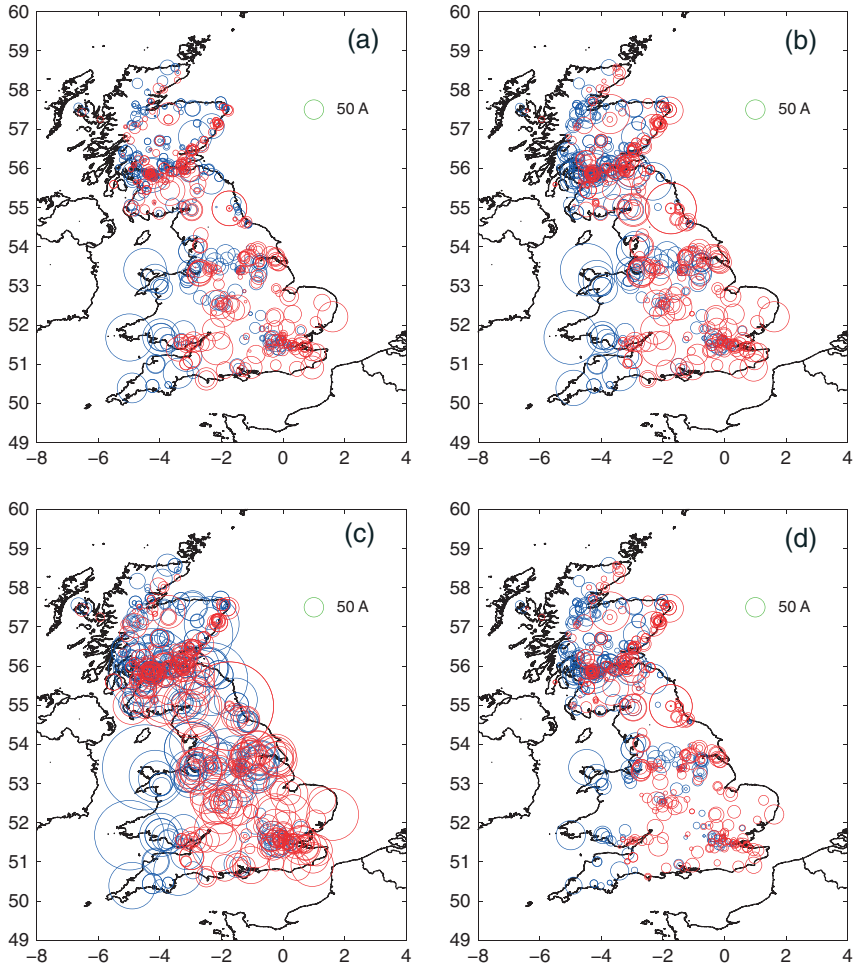

Figure 9. Snapshots of GIC in the National Grid GB high-voltage network due to an extreme storm scenario (approximately a factor of 5×) of the 30 October 2003 geomagnetic storm (due to an electric field with a period of 120 s). (a) Time: 19.30 h, (b) Time: 20.50 h, (c) Time: 21.20 h, and (d) Time: 22.50 h (see Figure 4). Blue indicated GIC directed into the grid, red indicates GIC into the ground. Circle size represents size (relative to scale). Note that many sites host multiple transformers.

use three discrete periods (120, 600, and 1800 s) only to approximate the full spectrum.

[29] The 2012 model of the UK network consists of 701 transformers and 1153 connections. Some connections are very short, for example, between two transformers on the same site, while the longest is 189 km. The median line length is 10 km (mean: 17 km). Figure 5 shows the UK 400 kV and 275 kV network and the 132 kV network in Scotland. Note that the GIC given at a "substation" needs to be divided by the number of transformers on site, which varies between one and six depending on the node in question.

3. Results of Electric Field and GIC Computation

[30] Using the "thin-sheet" approximation, the excess electric field is estimated for a large area around the UK from –12° to +2° longitude and from 50° to 60° latitude i.e., the area is 14° × 10° in size. This large area includes the shallow sea and deeper ocean, though excludes effects from mainland Europe. The model has a resolution of 1/12th of a degree in latitude and longitude (approximately 10 km cell size). This gives an electric field model for each magnetic field configuration for a given period (e.g., 120 s).

[31] The thin-sheet modeling code was run with the BGS2012 conductivity model using the auroral electrojet model configurations for the three different response frequencies (where applicable). Note that an East-West aligned magnetic field (i.e., the X component) generates the north-south aligned (i.e., Y component) electric field. We concentrate on results from the shortest period events (120 s) as these generate the largest GIC from our modeling technique.

Table 3. Largest 10 Modeled GIC in the GB Grid for a Tapered-Cosine Electrojet Profile for a Given Return Period and Orientation[a]

Return Period	30[b]		100[b]		200[b]	
	X	*Y*	*X*	*Y*	*X*	*Y*
Node #						
1	91.9	77.0	275.6	230.9	459.3	384.8
2	72.6	68.8	217.9	206.5	363.1	344.1
3	53.1	56.5	159.2	169.5	265.4	282.6
4	40.5	43.8	121.4	131.5	202.3	219.1
5	39.6	38.3	118.8	115.0	198.0	191.7
6	37.6	31.7	112.7	–68.1	187.8	158.5
7	34.4	26.3	103.3	–74.3	172.1	131.7
8	33.2	–29.5	99.7	–88.6	–168.9	–147.7
9	–35.5	–43.8	–106.5	–131.5	–177.4	–219.1
10	–45.2	–55.5	–135.6	–166.5	–226.0	–277.5

[a]*X* = North; *Y* = East (units: amperes).
[b]Return period in years.

[32] Figure 6 shows the output of the thin-sheet modeling for assumed 30, 100, and 200 year extreme events based on the idealized auroral electrojets. The modeled electric fields induced in the surface by a period of 120 s are for H_0 values of 450, 1350, and 2250 nT from various auroral electrojet configurations are plotted. The largest field changes induce the largest surface electric fields, reaching up to 15.1 V/km in Figure 6 (bottom right).

[33] In Figure 7, the results of the thin-sheet modeling for four snapshot times from the 1-in-200 year storm event are shown. The modeled electric fields induced in the surface by a period of 120 s for H_0 values of 3918, 4454, 9420, and 1454 nT, respectively. The figure shows the largest field changes induced reach up to 8.1, 10, 27.9, and 6.9 V/km in Figure 7. These electric field amplitudes are similar to those modeled in *Pulkkinen et al.* [2012].

[34] From the computed surface electric fields, GIC were obtained for each of the 701 transformers in the network for each extreme scenario. Figure 8 illustrates the GIC generated for a 100 year scenario for the 120 s period for the four configurations of the auroral electrojet. The GIC entering the grid are shown in blue (positive), while GIC exiting into the ground are in red (negative). Note that the sign of the GIC (positive or negative) is not important in terms of its impact on a transformer, as it is the absolute DC bias in the transformer that affects its performance.

[35] Figure 9 shows the modeled GIC generated for a 200 year scenario for the 120 s period from the four snapshots of the extreme storm of section 2.2.2 . The values are larger than those in Figure 8 which is to be expected as the magnetic field values are larger. Due to the spatial complexity of the magnetic field, the locations of large magnitude GIC differ from the hypothetical electrojet model.

[36] The results of the 10 largest GIC at the nodes are tabulated in Tables 3 (Tapered-Cosine profile) and 4 (Top-Hat profile). The tables show the output of the GIC model for each expected return period, depending on the orientation of the electrojet. (For commercial reasons, the identity of the nodes are not given.) Note that different nodes have the largest value of GIC, depending on the orientation of the electrojet and that the values from the Top-Hat profile are, on average, larger.

[37] The largest GIC occur in the north of the UK, and in the "corner" nodes of system (e.g., southwest Wales and England) or in isolated regions (Scottish Borders). Where nodes lie close together, especially in the southern UK, there is a tendency for smaller GIC (e.g., London/southeast England), though this is not necessarily the case in other clusters of transformers (e.g., northeast England). Also, due to the different transformer characteristics (e.g., from age, type, and connectivity), even nodes on the same site display different GIC susceptibility, indicating that the problem of understanding GIC even at a single site can be subtle.

[38] Although higher voltage power lines are most affected by GIC, we have found that including lower voltage lines does modify the electrical topology of the grid, changing the paths of least resistance for excess current. To illustrate this, we modeled the GIC in the 400 kV and 275 kV lines only and compared it to the GIC computed at the same transformers when the 132 kV grid in the northern UK is included. Figure 10 shows the differences at the common nodes using a Tapered-Cosine profile during a 100 year event for a 120 s period (i.e., the electric field from Figure 6). The largest differences for the East-West alignment of the electrojet (Figure 10a) are located in the north of the UK, vanishing in more southerly nodes. When the electrojet is north-south aligned (Figure 10b), the largest differences are up to about 8% of the total GIC at any given site. The number of nodes affected across the region also increases slightly, with nodes much further south of the 132 kV grid showing differences. This result suggests that any unmodeled connectivity of the high-voltage grid to lower voltage lines will have a modest effect on the size of GIC computed.

Table 4. Largest 10 Modeled GIC in the GB Grid for a Top-Hat Electrojet Profile for a Given Return Period and Orientation[a]

Return Period	30[b]		100[b]		200[b]	
	X	*Y*	*X*	*Y*	*X*	*Y*
Node #						
1	93.8	114.7	281.3	344.2	468.9	573.7
2	78.8	105.1	236.3	315.2	393.9	525.3
3	67.4	73.2	202.3	219.7	337.2	366.2
4	43.8	61.4	131.5	184.1	219.2	306.8
5	42.4	55.3	127.3	165.9	212.1	276.4
6	40.4	48.9	121.3	146.7	202.2	244.5
7	40.4	39.9	121.2	119.8	201.9	199.7
8	–37.1	–39.3	120.6	–117.9	200.9	–196.5
9	–42.4	–55.3	–127.3	–165.9	–212.1	–276.4
10	–55.7	–97.9	–167.2	–293.7	–278.7	–489.5

[a]*X* = North; *Y* = East (units: amperes).
[b]Return period in years.

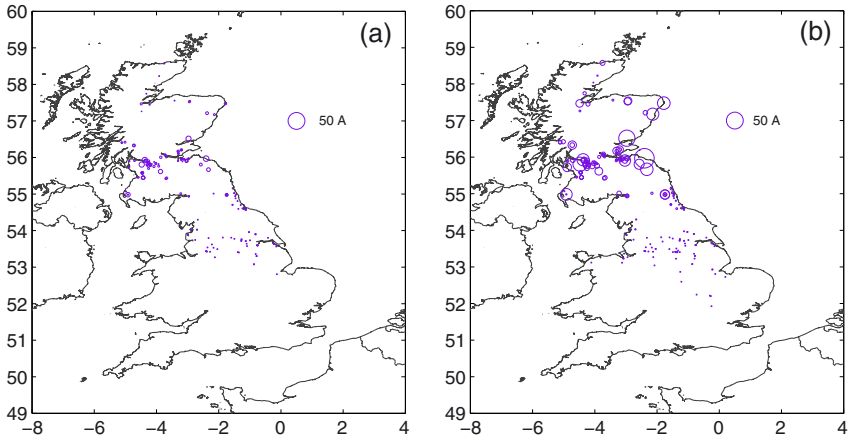

Figure 10. Differences in GIC in the 400 and 275 kV network when the 132 kV network is not included. GIC are due to a 100 year extreme scenario (120 s period) from an auroral electrojet with a Tapered-Cosine profile (c.f. Figures 8a and 8b): (a) East-West alignment and (b) North-South alignment. Circle size represents size (relative to scale). Note that many sites host multiple transformers.

4. Discussion

[39] We attempt to determine the flow of GIC in the UK power grid during the worst-case scenarios of space weather that can be expected in a 200 year period. The use of idealized electrojet models allows us to investigate the hypothetical response of the grid while a scaled version of the 2003 Halloween storm gives a more nuanced spatial magnetic field model.

[40] From a comparison of the magnetic field configurations in Figures 2 and 4, it can be seen that the Tapered-Cosine electrojet East-West alignment (Figure 2 (top left)) is arguably a more physically realistic distribution of electrical current in the ionosphere. However, the tapered-cosine electrojet results in typically lower GIC than the Top-Hat electrojet (in Figures 8c and 8d)).

[41] Although model outputs are described in terms of both East-West ("X") and North-South ("Y") scenarios, the dominant electrojet orientation is in the East-West (geomagnetic) direction, particularly over prolonged periods, though over shorter intervals there can be a strong north-south component. Any North-South component to the electrojet over the UK (e.g., during a westward traveling surge) will on average increase the GIC flowing in transformer earths. In places, this GIC can be an order of magnitude greater than that for an East-West oriented electrojet. Longer period variations with significant magnitude (e.g., > 3000 nT/min) are physically less realistic, as noted in section 2.2.1, but could produce large GIC if realized.

[42] Analysis of the spatial distribution of the magnetic field strength during large storms (e.g., October 2003) suggests that a single electrojet model is often not correct. For example, Figure 4 shows a complex magnetic field distribution for 21:20 during the peak of the storm. As well as a large variation in strength, the spatial variation gives rise to the largest GIC occurring in the central parts of the UK (Figure 9), rather than in northern regions (as occur in Figure 8).

[43] One of the more interesting aspects is that the largest GIC are positive (i.e., as the current enters the grid). This is due to the topology of the grid and the location of the nodes, as the current tends to flow from North to South. Due to the larger number of nodes in close proximity in the southern UK (where the population is densest), it appears the current flowing out is divided among a greater number of nodes.

[44] However, there are several limitations to this approach; for example, the geophysical model of the auroral electrojet is idealized, as it is assumed that the periodic variations in the auroral electrojet are concentrated into a discrete frequencies. This is unphysical but makes the problem manageable. We also assume that the electrojet parameters (location, width, and strength) from the analysis of 30 years of data [*Thomson et al.*, 2011] are reasonably representative during extreme events over longer time scales.

[45] The thin-sheet modeling approach has various physical constraints. Short period variations of less than 30 s cannot be correctly modeled using the thin-sheet method [*McKay*, 2003], as the assumptions for deriving skin depth break the approximation between conductivity and the period of the electromagnetic wave. In reality, very rapid changes of the magnetic field do not penetrate deeply into the ground. However, significant GICs have been measured during Sudden Storm Commencement events [*Kappenman*, 2003; *Liu et al.*, 2009], and these occasionally have pulse widths less than 60 s with rise times on the order of seconds. If the surface conductivity is very low to a depth of a few kilometers, these events can generate large electric fields for a short period of time.

[46] The power grid itself changes over time and even the model here is simplified with respect to the contemporary network. However, it should provide a good indication of grid response and our modeling does show that the same locations are consistently at risk from particularly large GIC. This can be used to inform network engineers of potential issues to monitor and allow planning and preparation to be made in the case of an extreme space weather event. During an actual event, measurement of the external magnetic field from local magnetic observatories can be used to provide near real-time estimates of GIC from simulations based on the conductivity and network models used in this study. To generate an electric field, an assumption about the dominant frequency of the measured magnetic field amplitude must be made. However, our method gives a fast assessment of likely hot spots in the system and can be run in near to real time to help in operations.

5. Conclusions

[47] We have investigated the generation of GIC in the high-voltage power network in the UK in response to 100 year and 200 year extreme geomagnetic storm scenarios. We have shown how a detailed model of the UK conductivity, based on the BGS 1:625000 geological database, can be used to generate surface electric field models from magnetic field changes induced by idealized auroral electrojet models.

[48] The GIC obtained show the theoretical response of the UK power system to an extreme space weather event. This will help transmission network engineers plan for and protect the grid from extreme events. Future improvements to the theoretical modeling will require validation of the outputs against real GIC measurements in the network during storm conditions.

[49] **Acknowledgments.** This research was partly funded by NERC New Investigators grant NE/J004693/1 and from the European Community's Seventh Framework Programme (FP7/2007–2013) under grant agreement 260330. The Sub-Auroral Magnetometer Network data (SAMNET) is operated by the Space Plasma Environment and Radio Science (SPEARS) group, Department of Physics, Lancaster University. We thank National Grid for their help in constructing a detailed network model. We wish to acknowledge the valuable comments from the two anonymous reviewers in improving the manuscript. This paper is published with the permission of the Executive Director of the British Geological Survey (NERC).

References

Amm, O., and A. Viljanen (1999), Ionospheric disturbance magnetic field continuation from the ground to the ionosphere using spherical elementary current systems, *Earth Planets Space*, *51*, 431–440.

Beamish, D., (2012), The 1:625k near-surface bedrock electrical conductivity map of the UK, *Tech. Rep. OR/12/037*, Br. Geol. Surv., 23 pp., Keyworth, Nottingham, U. K.

Beamish, D., and J. White (2012), Mapping and predicting electrical conductivity variations across southern England using airborne electromagnetic data, *Q. J. Eng. Geol. Hydrogeol.*, *35*, 99–110, doi:10.1144/1470-9236/11-026.

Beamish, D., T. D. G. Clark, E. Clarke, and A. W. P. Thomson (2002), Geomagnetically induced currents in the UK: Geomagnetic variations and surface electric fields, *J. Atmos. Sol. Terr. Phys.*, *64*, 1779–1792, doi:10.1016/S1364-6826(02)00127-X.

Erinmez, I. A., J. G. Kappenman, and W. A. Radasky (2002a), Management of the geomagnetically induced current risks on the national grid companys electric power transmission system, *J. Atmos. Sol. Terr. Phys.*, *64*, 743–756, doi:10.1016/S1364-6826(02)00036-6.

Erinmez, I. A., S. Majithia, C. Rogers, T. Yasuhiro, S. Ogawa, H. Swahn, and J. G. Kappenman (2002b), Application of modelling techniques to assess geomagnetically induced current risks on the NGC transmission system, in *International Council on Large Electrical Systems*, pp. 1–10, vol. 2002 Session, SC 39, Conseil International des Grands Réseaux Électriques (CIGRE), Paris, France.

Kappenman, J. (2003), Storm sudden commencement events and the associated geomagnetically induced current risks to ground-based systems at low-latitude and midlatitude locations, *Space Weather*, *1*(3), 1016, doi:10.1029/2003SW000009.

Kappenman, J. G. (2006), Great geomagnetic storms and extreme impulsive geomagnetic field disturbance events: An analysis of observational evidence including the great storm of May 1921, *Adv. Space Res.*, *38*(2), 188–199, doi:10.1016/j.asr.2005.08.055.

Lehtinen, M., and R. Pirjola (1985), Currents produced in earthed conductor networks by geomagnetically-induced electric fields, *Ann. Geophys.*, *4*, 479–484.

Liu, C.-M., L.-G. Liu, and R. Pirjola (2009), Geomagnetically induced currents in the high-voltage power grid in China, *IEEE Trans. Power Delivery*, *24*(4), 2368–2374, doi:10.1109/TPWRD.2009.2028490.

Mann, I., et al. (2008), The upgraded CARISMA magnetometer array in the THEMIS era, *Space Sci. Rev.*, *141*, 413–451, doi:10.1007/s11214-008-9457-6.

McKay, A. (2003), Geoelectric fields and Geomagnetically Induced Currents in the United Kingdom, PhD thesis, Univ. of Edinburgh, Edinburgh, U. K.

McLay, S., and C. Beggan (2010), Interpolation of externally-caused magnetic fields over large sparse arrays using Spherical Elementary Current Systems, *Ann. Geophys.*, *28*, 1795–1805, doi:10.5194/angeo-28-1795-2010.

Pulkkinen, A., E. Bernabeu, J. Eichner, C. Beggan, and A. Thomson (2012), Generation of 100-year geomagnetically induced current scenarios, *Space Weather*, *10*, S04003, doi:10.1029/2011SW000750.

Radasky, W. A. (2011), Overview of the impact of intense geomagnetic storms on the U.S. high voltage power grid, in *IEEE International Symposium on Electromagnetic Compatibility*, pp. 300–305, Inst. of Electr. and Electron. Eng., Washington, DC. doi:10.1109/ISEMC.2011.6038326.

Smith, P. (1990), Effects of geomagnetic disturbances on the National Grid System, *paper presented at 25th Universities Power Engineering Conference,* Aberdeen, U. K.

Thomson, A. W. P., A. J. McKay, E. Clarke, and S. J. Reay (2005), Surface electric fields and Geomagnetically Induced Currents in the Scottish Power grid during the 30 October 2003 geomagnetic storm, *Space Weather*, *3*, S11002, doi:10.1029/2005SW000156.

Thomson, A. W. P., E. Dawson, and S. Reay (2011), Geomagnetic extreme statistics for Europe, *Space Weather*, *9*, S10001, doi:10.1029/2011SW000696.

Turnbull, K. (2010), Modelling GIC in the UK, *Astron. Geophys.*, *51*(5), 25–26, doi:10.1111/j.1468-4004.2010.51525.x.

Turnbull, K. (2011), Modelling of Geomagnetically Induced Currents in the United Kingdom, PhD thesis, Univ. of Lancaster, Bailrigg, Lancaster, U. K.

Vasseur, G., and P. Weidelt (1977), Bimodal electromagnetic induction in non-uniform thin sheets with an application to the northern Pyrenean induction anomaly, *Geophys. J. R. Astron. Soc.*, *51*, 669–690.

Viljanen, A., and L. Häkkinen (1997), *IMAGE magnetometer network*, in *Satellite-Ground-Based Coordination Sourcebook,* SP-1198, edited by M. Lockwood, M. N. Wild, and H. J. Opgenoorth, p. 111, ESA Publications, Frascati, Italy.

Viljanen, A., H. Nevanlinna, K. Pajunpää, and A. Pulkkinen (2001), Time derivative of the horizontal geomagnetic field as an activity indicator, *Ann. Geophys.*, *19*, 1107–1118, doi:10.5194/angeo-19-1107-2001.